Experimental study on seismic performance of new-type composite shear wall

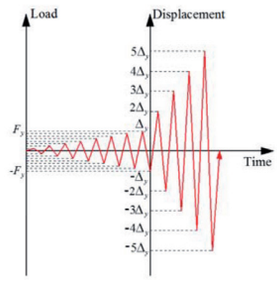

Estudio experimental sobre el comportamiento sísmico de un nuevo tipo de muro cortante compuesto

Xiaoruan Song, Chenglin Huang*, Guanfang Zhang, Wenchao Shan, Yongmeng Wang
School of civil engineering, North China University of Technology, Beijing 100144, China
* Corresponding author, e-mail: 594914390@qq.com

DOI: http://dx.doi.org/10.6036/9192 | Recibido: 01/04/2019 • Inicio Evaluación: 01/04/2019 • Aceptado: 10/06/2019

RESUMEN

- Un nuevo muro de cortante compuesto como producto industrializado es prometedor en la ingeniería civil. La aplicación en la construcción es limitada y no satisfactoria debido a la tremenda dificultad que supone la fabricación de los muros de cortante reforzados con mallazos y a la gran cantidad de acero usado en ellos. Este documento propone un nuevo tipo de muro de cortante compuesto, con un proceso de fabricación sencillo y un peso reducido. Las propiedades mecánicas de estos muros compuestos se han estudiado realizando experimentos cuasiestáticos en cuatro propuestas de muros de cortante compuestos y un muro de cortante de hormigón convencional. La influencia de la relación cortante-vano, la relación de carga axial y la conexión de las interfaces en los comportamientos sísmicos del muro compuesto, se incluyeron mediante el análisis de la capacidad portante, las curvas de histéresis, la degeneración de la rigidez, la ductilidad del desplazamiento, y la capacidad de disipación de energía. Los resultados muestran que el nuevo tipo de muro de cortante compuesto muestra un buen rendimiento sísmico y propiedades mecánicas similares a las del muro convencional; los anclajes de cizallamiento instalados en la interfaz entre la placa de cemento reforzado con fibra de vidrio prefabricada y el hormigón vertido in situ pueden mejorar el rendimiento de adhesión, la rigidez inicial y la capacidad de disipación de energía; el aumento de la relación de carga axial y la reducción de la relación de cortante-vano pueden mejorar la capacidad de carga del muro de cortante. Se ha desarrollado una fórmula para calcular la capacidad portante de la sección normal de estos muros de cortadura compuestos, que muestra un buen ajuste con los resultados de las pruebas. Este estudio puede servir de referencia para el diseño y las aplicaciones de ingeniería de los muros de cortante compuestos.
- **Palabras clave:** muro cortante compuesto, comportamiento sísmico, ensayo cuasiestático, unión de interfaces, anclajes de cizalladura9).

ABSTRACT

The composite shear wall structure is an industrialized and promising product in civil engineering. Its application in the industry is limted and not satisfying due to the tremendous difficulty in manufacturing the lattice reinforced shear walls and large amount of used steel. This paper proposes a new-type composite shear wall with easy fabrication process and decreased weight. The mechanical properties of the composite walls were studied by performing quasi-static experiments on four proposed composite shear walls and one conventional concrete shear wall. The influence of shear-span ratio, axial load ratio and interface connection on seismic behaviors of the composite structure were included by analyzing the bearing capacity, hysteresis and skeleton curves, stiffness degeneration, displacement ductility and energy dissipation capacity. Results show that the new-type composite shear wall shows good seismic performance and similar mechanical properties with the conventional wall; Shear studs installed at the interface between the precast fibergalss reinforced cement plate and cast-in-place concrete can improve the bonding performance, initial stiffness and energy dissipation capacity; Increasing the axial load ratio and reducing shear-span ratio can improve the bearing capacity of the shear wall. A formula was developed to calculate the bearing capacity of the normal section of such composite shear walls, which shows good agreement with the test results. This study may provide reference for design and engineering applications of the composite shear walls.

Keywords: Composite shear wall, Seismic performance, Quasi-static test, Interface bonding, Shear studs.

1. INTRODUCTION

The shear wall structure system is widely found in high-rise buildings because of its advantages in terms of integrity, the ability to sustain external loads and the seismic performance. At present, the on-site pouring method is commonly used for construction of the shear wall structure. This technique, however, is far more labor-intensive, time-consuming and not environment-friendly. It also consumes a large amount of construction materials such as steels and woods. As an alternative, the precast structure shortens the construction period and saves materials at the same time. It soon becomes one of the most popular techniques (for fabricating the shear wall structure). However, the connection between different precast components still remains the major issue and the overall integrity of the precast structure needs to be improved. Furthermore, the precast structure hardly presents the same seismic performance as its cast-in-place counterpart. Therefore, this structure is mainly found in civil buildings at low seismic fortification intensity zones.

In recent years, scholars have begun their research on the composite shear wall structures to further improve the overall performance. The composite shear wall first started in Germany

and soon gained its popularity in Europe and Japan. It consists of the precast concrete plates at both sides and the cast-in-place concrete in the middle. Generally, the composite shear wall shows the advantages of both the precast and cast-in-place shear walls, i.e. allowing installation errors during construction, simplifying the component assembly and improving the construction efficiency [1]. Therefore, the bonding properties of the interface between the precast plates and cast-in-place concrete become more important since they have a major influence on the overall performance of composite shear wall. Currently, the interface lattice steel is commonly installed at the precast concrete plates and functions to increase the bonding performance, yet its application in the industry is still limited due to the enhanced complexity of fabrication, increased amount of used steel and consequently improved volume and weight of the precast plate [2-3].

Hence, it is necessary to improve the bonding performance of the composite shear wall, simplify the fabrication process and reduce the weight of the precast plate. To this end, a new-type composite concrete shear wall structure is proposed in this study and experimental tests are performed to study the seismic and bonding performance. This paper attempts to provide references for design and engineering application of the new-type composite shear wall.

2. STATE OF THE ART

The experimental tests on mechanical behaviors of composite shear walls have been extensively performed in previous studies. Generally, the composite samples were mostly placed under the axial and lateral loading conditions for investigating the mechanical performance. Frankl et al. conducted the axial and cyclic horizontal loading tests on a total of six composite shear walls using prestressed steel bars as the shear connector to improve bonding performance. They concluded that the shear connectors at the interface have a major impact on the deformation and stiffness of the composite structures, and that the carbon fiber reinforced polymer (CFRP) shear connector is able to effectively transmit the shear force [4]. Mohamad et al. prepared six precast light-weight foam-concrete composite shear walls and they concluded from the axial loading test that the bearing capacity of the composite samples are close related to the confinement on the bottom wall and the strength of the foam concrete [5-6]. Benayoune et al. found that the precast plates at both sides and the cast-in-place concrete in the middle could work together to sustain external loads by performing axial and eccentric loading tests. A nonlinear positive relationship was found between the bearing capacity and the height-to-thickness ratio of the composite shear wall [7-8].

A seismic design is required for the shear walls because of the earthquake activities. Therefore, the test on seismic performance of the composite shear wall is a major concern and also a prerequisite for the application of the structure in the industry. The seismic performance of composite shear walls has been documented in previous studies by a number of researchers. Ye et al. carried out the quasi-static tests on composite shear walls with different axial load ratios and found out that an increase in axial load ratio can restrict the crack initiation and propagation and improve the bearing capacity [9]. Bagheri and Oh proposed an optimization formula for calculating the distribution of the yield shear force coefficients of energy dissipation devices under seismic loading [10]. Beko et al. found that the sequence of load cycle amplitudes at the quasi-static rate shows no significant influence on ultimate strength or overall behavior of the wall [11]. Wang et al. utilized the confined member at both sides of the sample to increase bonding between precast plates and cast-in-place concrete and improve the overall seismic performance [12]. Wang et al. concluded that the concealed steel plate bracing can be used to improve the bearing and deformation capacity as well as the ductility of the composite shear wall by performing quasi-static tests on 2 local high damping composite shear walls [13]. Chu et al. proposed a new composite shear wall with rough plate-concrete interface or key slots at the interface. To some extent, the proposed composite structure improves the bonding performance of the interface [14].

Efforts to improve the interface connection between the plate and concrete have been studied for years. Previous studies have shown that both the addition of shear connectors at the interface and a key slot design at the interface improve the bonding and seismic performance of the composite shear wall. This is because the shear connector or key slots function to ensure that the precast shear plates and cast-in-place concrete cooperate to sustain external loads. However, the fabrication of the precast concrete plates with shear connector is too complicated for engineering application, and the key slot design requires a thicker precast plate of approximately 50 mm at both sides. As a result, the composite shear wall is not cost effective or technologically advanced due mainly to the large amount of used steel and the improved size and weight of the precast plates. Generally, a better design of the composite shear walls considers both the bearing capacity and the overall dimensions and weight of the precast plates.

Based on previous studies on the fiber reinforced cement plates [15-16], in this work, the authors propose a new-type composite shear wall consisting of two 10-mm thick precast fiberglass mesh reinforced cement plates at both sides and the self-compacting concrete in the middle between the plates. The authors have performed the quasi-static tests on four of the prepared composite shear walls in this paper to investigate the influence of shear-span ratio, axial load ratio and interface connection methods on the seismic behaviors. This is also compared with one conventional shear wall under the same loading conditions. The mechanical and seismic performance, deformation and failure characteristics of the samples are analyzed and discussed to provide insights for future design and application of such composite shear walls. This study is organized as: Section 3 describes the quasi-static test method of composite shear walls. Section 4 gives the analysis and discussion of the test results. Conclusions are summarized in Section 5.

3. METHODOLOGY

3.1. SPECIMEN PREPARATION

Five specimens with different parameters were prepared in this study, including four composite shear walls (CSW1, 2, 3 and 4) and one conventional shear wall (W5). Fig. 1 and 3 gives the schematics of the samples showing the overall structures and dimensions. The specimen consists of the top and base beams, and the composite samples with two 10-mm thick fiberglass mesh reinforced precast plates at both sides and a 100-mm thick cast-in-place self-compacting concrete between the plates. The cross-sectional size of the base and top beams are 400×400 mm and 180×250 mm (width and height), respectively, and the composite shear wall is 1000 mm high, 600 mm wide and 120 mm thick (Note that the width of CSW1 is 800 mm). The samples are used to study the influence of important parameters including the shear-span ratio,

the axial load ratio and interface connection on the seismic performance of the shear walls (see Table I). The interface connection methods include a natural bonding between the plate-concrete interface and the mechanical connection using studs. For the natural bonding sample, the rough surfaces of the precast plate to provide friction for the bonding interface, while the mechanical bonding samples having the 8-mm diameter studs cutting through the precast plate and extending 50 mm into the cast-in-place concrete. The placement of the studs on CSW4 can be found in Figs. 1b and 2.

The specimens were prepared exactly according to the Chinese code for seismic design of building (GB50011-2010) and the Chinese technical specification for concrete structures of tall building (JGJ3-2010). The C35 concrete is used for construction of the base beam, while self-compacting concrete SC30 is used for the composite structures and top beam. The longitudinal bars and reinforcement stirrups of the base beam are designed as 14B18 and A8@150, respectively, while the composite structures utilize the 10B8 design for the 800-mm thick specimen and the 6B8 design for the 600-mm thick specimen, and the horizontal bars are designed as A6@100. The wall has two concealed columns (4B12 for the longitudinal bars and A6@100 for the horizontal bars) at both sides of the wall. The longitudinal bars and reinforcement stirrups of the top beam are designed as 6B12 and A8@150, respectively. The dimensions of the specimens and placement of the reinforcement bars are given in Fig. 3 (See section: supplementary material).

Fig. 4 (See section: supplementary material) gives a schematic of the precast plate that is composed of the cement mortar and two layers of fiberglass mesh. The cement mortar is a mixture of the low alkalinity cement, coal flyash, expanded perlite, sand, water reducing admixture and coupling agent with a proportion of 1:0.25:0.015:0.15:0.007:0.015 by weight. The mesh size is 5 × 5 mm^2 with a thickness of 0.65 mm. The manufacturing process of precast plate is shown in Fig. 5 (See section: supplementary material).

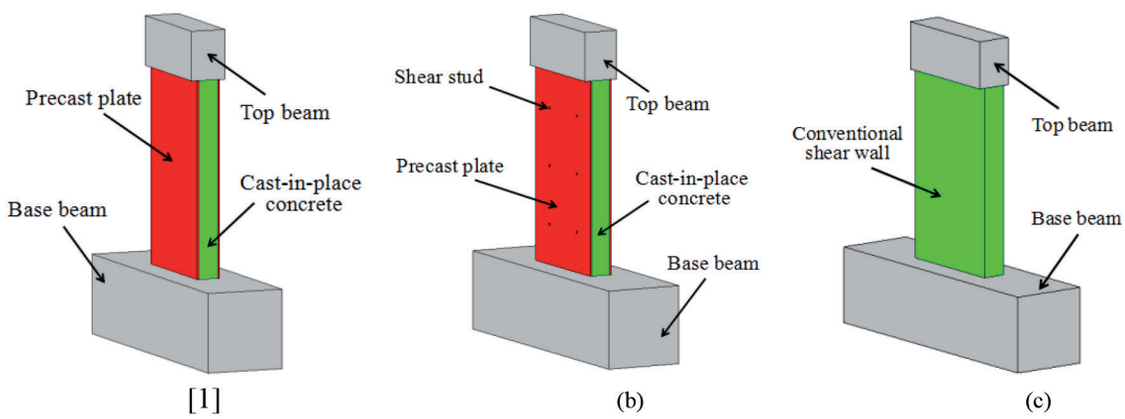

Fig. 1. The schematics of the specimens. (a) CSW1-3, (b) CSW4, (c) W5

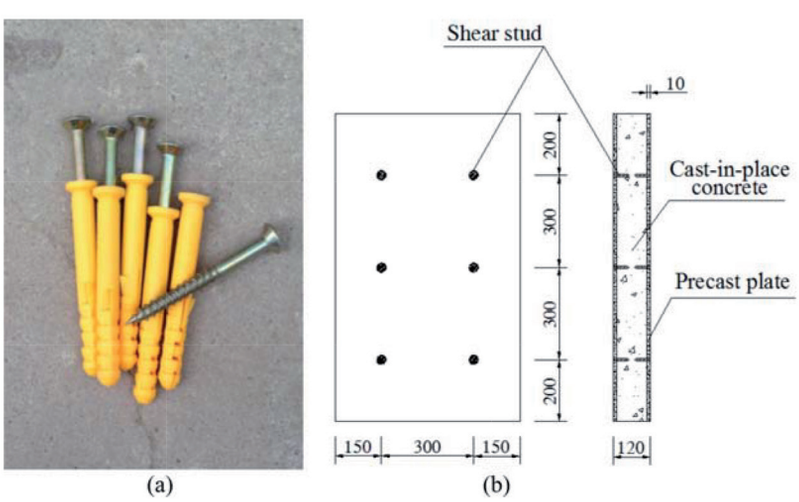

Fig. 2. (a) Shear stud, (b) The placement of shear studs on the composite shear wall

The standard concrete cubes (150 × 150 × 150 mm^3) and prismoids (150 × 150 × 300 mm^3) were prepared to obtain the actual strength, which are shown in Table II (See section: supplementary material). Table III (See section: supplementary material) also lists the mechanical properties of the steel bars used in the composite sample.

3.2. LOADING AND MEASURING

The tests were carried out on a multi-functional loading machine. The maximum vertical and horizontal loads that can be provided are 5000 kN and 1000 kN, respectively. The setup of the composite sample on the loading machine is shown in Fig. 6. The axial load was applied to the top beam by No. 1 hydraulic jack.

Specimen	Height (mm)	Width (mm)	Thickness (mm)	Shear-span ratio	Axial load ratio	Interface connection
CSW1	1000	800	120	1.25	0.1	Natural contact
CSW2	1000	600	120	1.67	0.1	Natural contact
CSW3	1000	600	120	1.67	0.2	Natural contact
CSW4	1000	600	120	1.67	0.2	Shear studs
W5	1000	600	120	1.67	0.2	-

Table I Important parameters of specimens

A 20-mm thick steel plate is placed between the top beam and the vertical hydraulic jack to create a uniform distributed stress on the composite sample. The axial load was maintained constant through the test. Substituting the designed axial load ratios (see Table I) into Eq. 1 yields the axial load:

$$n = \frac{1.25N}{f_c A_c / 1.4 + f_y A_s / 1.1} \quad (1)$$

where n is the axial load ratio from Table I; N is the axial load; f_c is the compressive strength of the cast-in-place concrete; A_c is the cross-sectional areas of the shear wall; f_y is the yield strength of longitudinal bars in the wall; A_s is the total cross-sectional areas of longitudinal bars in shear wall. The numerical values 1.4 and 1.1 are the material reduction coefficients of concrete and steel bars, respectively. 1.25 is the load safety factor according to the Chinese code for design of concrete structures (GB50010-2010).

On the horizontal direction, the low-frequency cyclic load was applied on the center of the top beam by No. 2 hydraulic jack fixed on the reaction wall. The horizontal loading procedure is shown in Fig. 7. It shows a two-step cylic loading scheme. The first step is a load control mode increasing from 0 at an increment of 20 kN prior to yield load of the sample, while a displacement control mode is used after yield at an increment of Δ_y, where Δ_y is the displacement at yielding, *and* F_y is the yield load corresponding to Δ_y. The experiment ceases when the load drops to 85% of the peak load.

As shown in Fig. 8 (See section: supplementary material), a total of five displacement sensors were placed on the shear wall. Of those, sensor D1 was installed at the center of the top beam, while sensors D2, D3 and D4 were evenly placed at the top, middle and bottom of the sample wall, respectively, for measuring horizontal displacement. Sensor D5 at the base beam was used for monitoring the foundation slippage. A number of strain gauges were embedded on the surface of the reinforcement bars or pasted on the surface of the shear wall. Loads, displacements and strain were recorded by an IMP data gathering system.

4. RESULTS AND ANALYSIS

The mechanical behaviors and properties of the composite samples were included in this section, including the failure characteristics, bearing capacity, hysteresis curve, skeleton curve, stiffness degeneration, ductility and energy dissipation. The equations for calculating the normal section bearing capacity of the shear wall were also derived by analyzing its equilibrium.

4.1. FAILURE CHARACTERISTICS OF SPECIMENTS

The progressive failure of the specimens during the test is similar. During the initial loading stage, the specimen stays in the elastic phase and no cracks are shown on the shear wall. The first crack typically occurs in horizontal and appears at the bottom of the shear wall. The further increase of the horizontal load sees the initiation of new cracks, and the extension and coalescence of the previous cracks. After the yielding of the sample, the horizontal cracks grow and incline to the center of shear wall, with an angle of 45-60° from the horizontal direction. More inclined cracks are observed on the central part of the shear wall at fracture the increasing horizontal loading, and these cracks are approximately symmetry to the centerline. At the final loading stage, the concrete on the bottom of the wall at both sides are crushed,

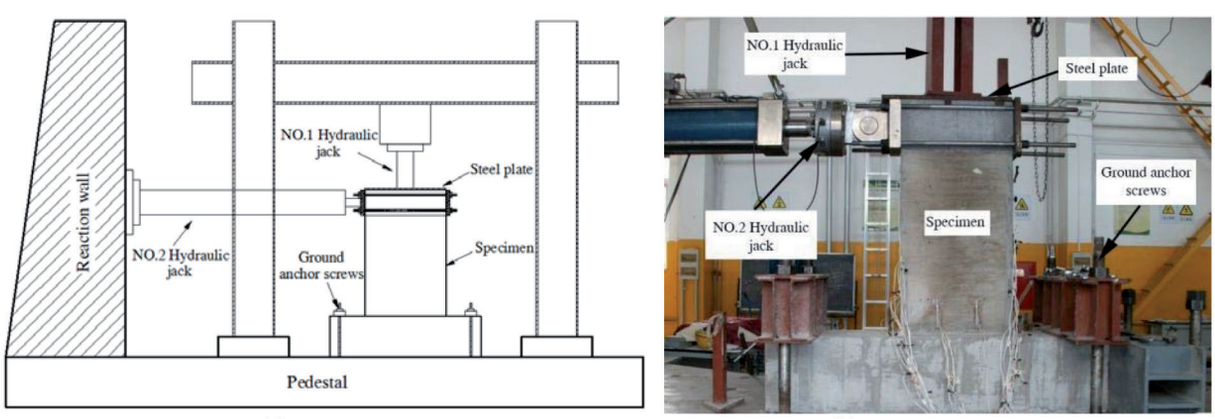

Fig. 6. Setup of the composite sample on the test machine. (a) Schematic, (b) Photograph

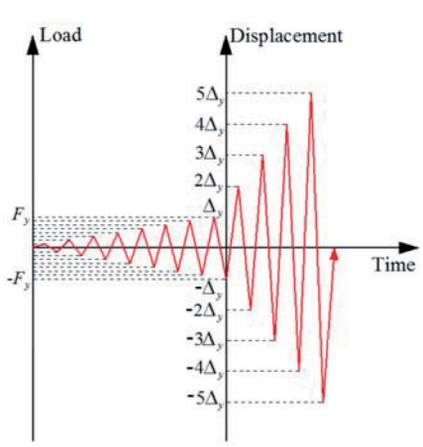

Fig. 7. The two-step horizontal cyclic loading procedure

as shown in Fig. 9. The test ceases when the horizontal load reduces to a level of 85% of the peak load, and the distribution of the fractures on the shear wall are shown in Fig. 10 (See section: supplementary material).

By comparing the failure characteristics of the composite and conventional shear walls (Fig. 10, See section: supplementary material), it is observed that more cracks appear on the composite walls, and the widths of the cracks tend to be smaller. The precast plate remains relatively intact, except some crashed concrete blocks found at the bottom of the composite shear wall. By contrast, most part of the conventional shear wall is crashed with larger size of failure concrete blocks at the wall foot.

The dislocation of one side of the precast plate from the cast-in-place concrete is also found for both the CSW2 and CSW3 sam-

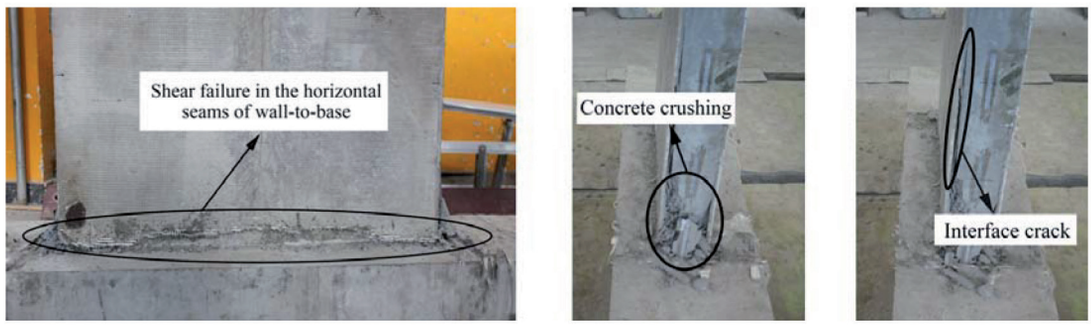

Fig. 9. Final failure modes of typical specimen. (a) Shear failure, (b) Crushing, (c) Interface crack

ples, and surface voids are observed on the exposed cast-in-place concrete, which indicates the poor natural-contact bonding performance of the plate-concrete interface. As a result, the sparsely-distributed cracks are observed on the surface of the dislocated plates, compared with the dense cracks on plates of the CSW1 and CSW4 samples with intact bonding between the plate and cast-in-place concrete. The precast plates and the cast-in-place concrete can work together to take the external loads. On the other hand, it is noted that the natural contact of the plate-concrete interface may sometimes provide good bonding performance yet have low reliability. The shear studs installed at the interface might be a more reliable alternative to pursue a good bonding behavior and avoid the dislocation.

4.2. MECHANICAL PROPERTIES

The load and displacement of the samples at the important loading stages are listed in Table IV (See section: supplementary material), in which F_c, F_y, F_m and F_u are the initial cracking load, yield load, peak load and ultimate load for specimens, respectively; Δ_c, Δ_y, Δ_m and Δ_u are the displacement corresponding to F_c, F_y, F_m and F_u. It is found that the low shear-span ratio sample (CSW1) has significant higher load values than the high shear-span ratio one (CSW2). Sample CSW3 with an axial load ratio of 0.2 presents a 16%, 14% and 12% higher of loads at the first crack, yielding point and peak point, respectively, compared with the sample CSW2 at the axial load ratio of 0.1. At the same shear-span ratio and axial load ratio, the sample CSW4 with shear studs at the interface, however, shows very similar peak load with the conventional shear wall W5, which is 6% higher than the natural-contact bonding sample CSW3. Hence, shear studs can improve the bonding performance between precast plates and cast-in-place concrete thus enhance the bearing capacity of composite shear walls.

4.3. HYSTERESIS CURVE

The load-displacement hysteresis curves for all the specimens are shown in Fig. 11. The load-displacement relationship plotted in Fig. 11 show that the hysteresis curves are found to be straight lines at the initial loading stage and no residual deformation remains after the unloading. The stiffness of the samples decreases after the crack initiation. The samples enter from the elastic to the elastic-plastic stage with larger residual deformation and areas of hysteresis loop with the increase of horizontal loading. The bow-shaped hysteresis curves are then observed at further development of the inclined cracks. After the yielding of the longitudinal bars at the concealed columns, the stiffness degeneration is more notable and the effect of pinching in the hysteresis loop is shown. The load declines gradually for all the composite shear walls following the peak load, indicating that the composite walls present a better horizontal loading capacity, energy dissipation capacity and ductility.

The hysteresis curve of the sample CSW4 with shear studs has a similar shape with the conventional sample, and more fuller compared with the natural-contact sample CSW3. This is because the shear studs may enhance the bonding properties of the plate-concrete interface; the integrity of the composite shear wall is therefore improved.

4.4. SKELETON CURVE

Fig. 12 (See section: supplementary material) gives the skeleton curves for all the specimens. The skeleton curves indicate a linear relationship between the load and displacement at the beginning of loading. After the appearance of the cracks, the stiffness as well as the slope of the skeleton curves reduces gradually. The curves decrease smoothly and show good ductility following the peak load. Sample CSW1 (low shear-span ratio) shows approximately 55% higher in load capacity than the high shear-span ratio counterpart CSW2, but its deformation performance is much poorer represented by the smaller displacement after yielding. Samples CSW2 and CSW3 show larger displacement at failure than the rest, which might due to (the fact that) the dislocation of the plates essentially reduces the effective thickness of the shear wall. Samples CSW4 and W5 have the most close curves, indicating that the shear studs can make the precast plates and the cast-in-place concrete work well together.

4.5. STIFFNESS DEGENERATION

The secant stiffness of the envelope curves at each loading/displacement level is adopted to describe the stiffness degradation behavior, which can be calculated from Eq. 2 [17-19].

$$K_i = \frac{|+F_i| + |-F_i|}{|+\Delta_i| + |-\Delta_i|} \tag{2}$$

where K_i is the stiffness of the specimen at *i*th load/displacement level, $+F_i$ ($-F_i$) is the positive (negative) peak load at *i*th load/displacement level, respectively, and $+\Delta_i$ ($-\Delta_i$) is the displacement corresponding to the positive (negative) peak load at *i*th load/displacement level, respectively.

Fig. 13 shows the stiffness degeneration curves for each specimen, from which we can see that the stiffness degeneration curves can be identified into two stages. The first stage starts from the initiation of cracks to yielding of the sample, which is characterized by the rapid degeneration of the stiffness. The stiffness degeneration in the second stage continues but the rate of degeneration reduces gradually to a nearly flat level. It is also noted that the sample CSW1 has the noticeably largest initial stiffness,

but its stiffness decay rate is also faster. The shear studs bonding sample CSW4 shows much higher initial stiffness compared with the natural contact bonding sample CSW3, while the samples CSW4 and W5 at the same shear-span ratio and axial load ratio have the most similar degeneration curves except that the initial stiffness of CSW4 is much higher, indicating that the precast cement plates and cast-in-place concrete may work together as one like the conventional concrete shear wall.

4.6. DUCTILITY AND ENERGY DISSIPATION

The ductility coefficient (μ) is an important index for evaluating the ductility performance of the structure, which can be calculated from Eq. 3. The ductility coefficients for each sample are given in Table IV. [20-21]:

$$\mu = \frac{\Delta_u}{\Delta_y} \tag{3}$$

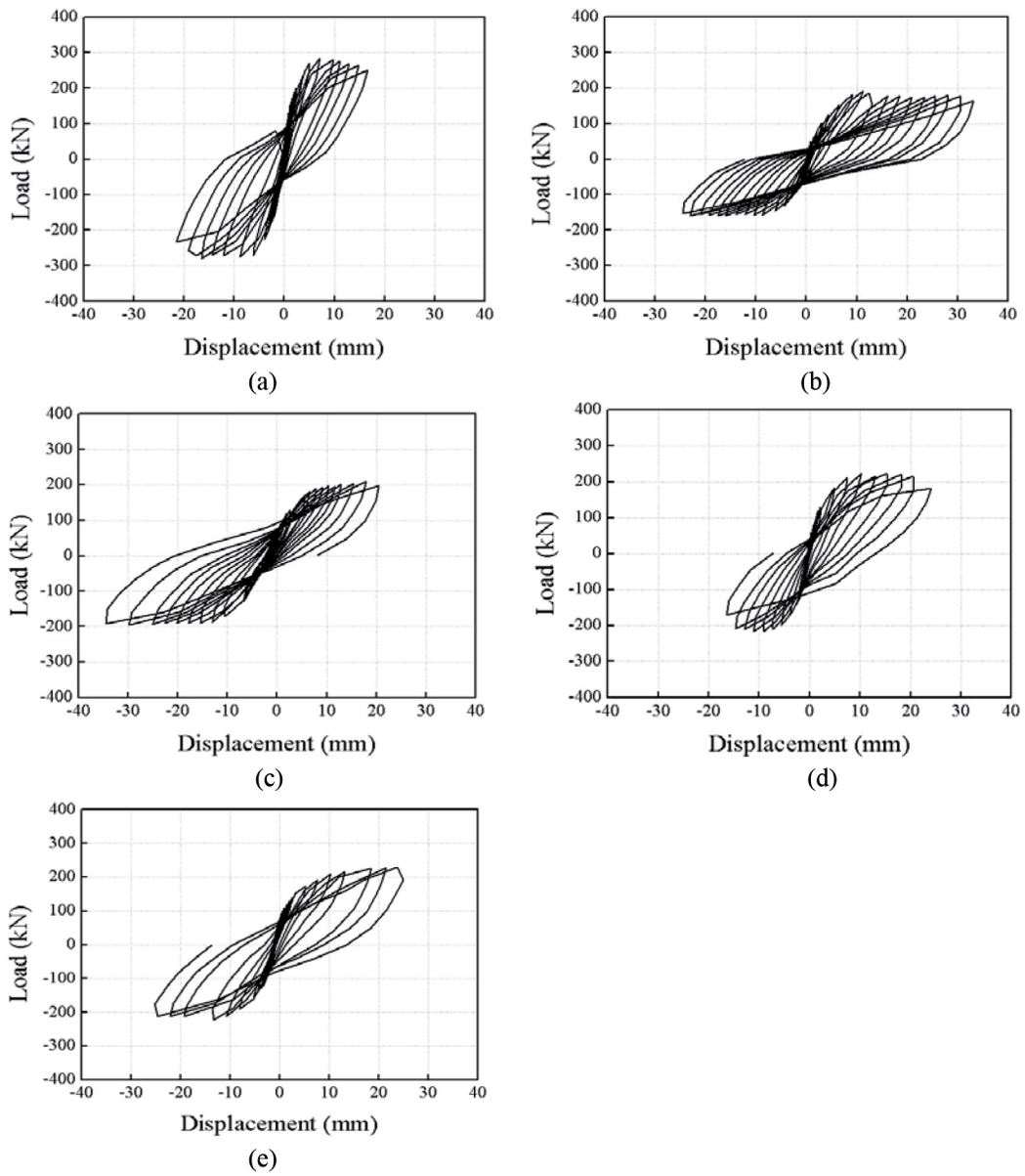

Fig. 11. Load-displacement hysteresis curves of the samples. (a) Specimen CSW1, (b) Specimen CSW2, (c) Specimen CSW3, (d) Specimen CSW4, (e) Specimen W5

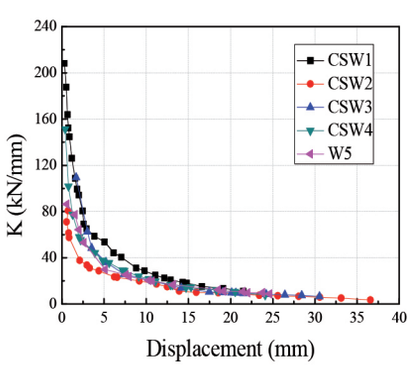

Fig. 13. Stiffness degeneration curves of the samples

where Δ_u is the ultimate displacement and Δ_y is the yielding displacement.

It is found that the ductility coefficients for all the five specimens are larger than 5, indicating the good ductility performance. Specifically, the four composite shear walls are larger in ductility factors than the conventional shear wall. For the composite shear walls, however, the low shear-span ratio sample CSW1 and the shear stud bonding sample CSW4 show the smaller ductility coefficients, corresponding to their smaller displacement. The low axial load ratio sample CSW2 shows the largest displacement and ductility coefficient.

The energy dissipation coefficient (*E*) is an important indicator representing the seismic performance of the structure. According to Fig. 14 (See section: supplementary material), the energy dissipation coefficient (*E*) is calculated by Eq. 4 and given in Table IV [22].

$$E = \frac{S_{(ABC+CDA)}}{S_{(\Delta OBG+\Delta ODH)}} \quad (4)$$

The sample CSW2 has the least energy decapitating coefficient of 1.71, while an increase of the axial load ratio (sample CSW3) and a decrease of the shear-span ratio (sample CSW1) can improve the decapitating coefficients to 1.81 and 1.98, respectively. Samples CSW3 and W5 have the similar energy decapitating coefficients at 1.81 and 1.85, respectively, indicating the similar energy decapitating capacity. The largest coefficient is found at 2.13 for sample CSW4, meaning that the shear studs installed at the interface enhance the energy decapitating capacity of the shear wall.

4.7. BEARING CAPACITY CALCULATING

The failure modes of the shear wall can be classified into compression failure with large and small eccentricity. According to the plane-section assumption, the stress is linearly distributed along the longitudinal section of the wall when subjected to both axial load and bending moment. Therefore, the ratio of the nominal compression height of the section over the effective height of the shear wall can be used to determine whether the failure modes is in large or small eccentric compression. A preliminary investigation of the samples after test implies that the five shear walls in this study shows compression failure with large eccentric compression, which is therefore discussed below.

When the sample is at compression with large eccentric compression, the longitudinal bars away from the neutral axis can approach the yield strength, while the longitudinal bars close to the axis are subjected to smaller stress, which is not considered in the calculation. The stress on the concrete in the compression zone reaches the limit compression strength. Fig. 15 (See section: supplementary material) gives a schematic of the mechanical model for the composite shear wall with large eccentric compression. For simplification, it is assumed that the longitudinal bars in the tensioned concealed column and the vertical distribution reinforcing bars within the range of (h_w-$2a_s$-*1.5x)* are yielded in tension zone (note that h_w is the height of the section of the shear wall, *x* is the nominal compression height, and a_s is the distance from the resultant point of tensile and compressive reinforcement bars to the closer edge of the section, Fig. 15); the longitudinal bars in the compressed concealed column yield; and the vertical distribution bars within the range of *1.5x* are not considered in the calculation. Yet the tensile strength of the fiber mesh within the range of (h_w -*1.5x)* is included [23].

Using the equations of equilibrium, the force equilibrium in the vertical direction is given in Eq. 5 and the moment about the centroid of the concrete compression section is given as Eq. 6.

$$N = N_c + A'_s f'_y - A_s f_y - N_{sw1} - N_{sw2} \quad (5)$$

$$N(e_0 - \frac{h_w}{2} + \frac{x}{2}) = A'_s f'_y \left(\frac{x}{2} - a_s\right) + A_s f_y \left(h_w - a_s - \frac{x}{2}\right) + M_{sw1} + M_{sw2} \quad (6)$$

The following equations provide the expression for each symbol given in Eqs. 5 and 6.

$$N_c = \alpha_1 f_{c1}(b_w - 2b_m)x + 2\alpha_1 f_{c2} b_m x \quad (7)$$

$$N_{sw1} = \frac{A_{sw} f_{yw}}{h_w - 4a_s}(h_w - 2a_s - 1.5x) \quad (8)$$

$$N_{sw2} = nh' f_{c2} \frac{E_b}{E_c}(h_w - 1.5x) \quad (9)$$

$$M_{sw1} = \frac{A_{sw} f_{yw}}{h_w - 4a_s}(h_w - 2a_s - 1.5x)\left(\frac{h_w}{2} - a_s + \frac{x}{4}\right) \quad (10)$$

$$M_{sw2} = nh' f_{c2} \frac{E_b}{E_c}(h_w - 1.5x)\left(\frac{h_w}{2} + \frac{x}{4}\right) \quad (11)$$

where *M* and *N* are the bending moment and sectional axial force of the composite shear wall; N_c is the sectional axial force of the concrete strip in the compression zone. N_{sw1} *and* M_{sw1} are the tensile force and the bending moment of the longitudinal distribution reinforcing bars within the range of (h_w-$2a_s$-*1.5x)*. N_{sw2} and M_{sw2} are the tensile force and the bending moment of fiberglass mesh within the range of (h_w-*1.5x)*. A_s and A'_s are areas of the tensile and compressive bars in concealed column, respectively; f_y and f'_y are the tensile and compressive yield strengths of reinforcement bars in concealed column; e_o is the eccentric distance computed as e_o=*M*/*N*; α_1 is the ratio between the stress of the rectangular stress diagram for the compressive concrete and the designed axial compressive strength of the concrete, which α_1=*1* is given as when the concrete strength is less than C50; f_{c1} and f_{c2} are the compressive strength of the cast-in-place concrete and precast plate; b_w and b_m are the thickness of the shear wall and the plate; A_{sw} is the total area of the longitudinal distribution steel bars; f_{yw} is the yield strength of the longitudinal distribution steel bars; *n* is numbers of the fiberglass mesh layers; *h'* is the thickness of a single fiberglass mesh; E_c is the elasticity modulus of the cement mortar used for the precast plates, E_c=*3x10*^{4} MPa; E_b is the modulus of the fiberglass mesh, E_b=*7.3x10*^{4} MPa.

The normal section bearing capacity of the composite shear wall estimated from the above equations is given in Table V (See section: supplementary material), and is compared with the experimental results. The calculated values are about 80% of the experimental, indicating a reasonable safety margin.

5. CONCLUSIONS

To study the seismic performance of a new-type composite shear wall, the quasi-static tests on the four composite shear walls and one conventional shear wall were carried out. The equations for computing the normal section bearing capacity of the composite shear wall were proposed. The conclusions are listed as follows.

(1) The composite shear wall comprising precast plates and the cast-in-place concrete presents good seismic performance under the quasi-static test. More cracks are observed on the composite shear walls at failure than the conventional shear wall, and the crack widths on the composite walls are smaller compared with the large cracks on the conventional wall. The precast fiber-reinforced cement plates of the composite shear wall remain relatively intact during the failure stage, and small pieces of broken concrete blocks are found falling on the bottom of the wall, while the conventional

concrete wall sees the crushed failure at majority part of the wall. Therefore, the precast fiber-reinforced cement plates may improve the integrity of the wall when subjected at loading.

(2) The composite shear walls have good seismic performance similar to the conventional wall. Both walls show similar load bearing capacity, hysteresis curve, skeleton curve, stiffness degeneration, displacement ductility and energy dissipation capacity, indicating that the precast plates and the cast-in-place concrete may work well together. The shear studs installed at the interface between the precast plates and the cast-in-place concrete may improve the bonding behavior, initial stiffness and energy dissipation performance of the shear wall. The seismic performance of composite shear wall with shear studs is most close to the conventional sample, indicating the good integrity of the precast plates and cast-in-place concrete.

(3) The composite sample with a small shear-span ratio shows high bearing capacity and initial stiffness but low deformation capacity and quick stiffness degeneration. Increasing the axial load ratio can not only increase the cracking load, yield load and peak load, but also improve the energy dissipation capacity of composite shear wall.

(4) The equations for calculating the normal section bearing capacity are proposed by analyzing the equilibrium of the shear wall. The calculated results are 20% less than the test results, indicating a reasonable safety margin. Therefore, the formula can be used to approximate the bearing capacity of the composite shear wall.

This work studies the feasibility of the novel composite shear wall by comparing the seismic performance with a conventional shear wall and provides a reference for future design of this kind of composite wall. The authors believe that the bonding between the precast plates and the cast-in-place concrete may largely influence the mechanical behaviors of the composite shear wall. The current study only considers the shear studs and the natural connection at the interface. The future work requires the study of the dimension and location of the shear studs or other better interface connection types on the mechanical properties of the composite shear wall.

REFERENCES

[1] Yang LP, Yu SL, Zhang QL, Cui JC. "Research status quo and key issues in superimposed shear wall structure". Building Structure. June 2017. Vol. 47-12. p. 78-88. DOI: http://dx.doi.org/10.19701/j.jzjg.2017.12.014

[2] Anghel LG, Anglart H. "Wall temperature prediction in annular geometry during post-dryout heat transfer". Journal of Power Technologies. June 2014. Vol. 94. p. 1-7

[3] Yao G, Xu CC, Yang Y, Wang MP, Zhang M, Thabeet A. "Working mechanism of a high-performance tower crane attached to wall joints". Journal of Engineering Science and Technology Review. March 2018. Vol. 11-1. p. 19-27. DOI: https://doi.org/10.25103/jestr.111.03

[4] Bernard AF, Gregory W, Tarek KH, Sami HR."Behavior of precast, prestressed concrete sandwich wall panels reinforced with CFRP shear grid". PCI Journal. March 2011. Vol. 56-2. p. 42-54. DOI: http://dx.doi.org/10.15554/pcij.03012011.42.54

[5] Noridah M, Wahid O, Redzuan A. "Precast lightweight foamed concrete sandwich panel(PLFP) tested under axial load: preliminary results". Advanced Materials Research. May 2011. Vol. 250-253. p. 1153-1162. DOI: http://dx.doi.org/10.4028/www.scientific.net/AMR.250-253.1153

[6] Samsuddin S, Ahmad I, Goh WI, Mohamad N, Samad AAA, Rahman MHA. "Structural behaviour of precast lightweight foamed concrete sandwich panel (PLFP) with double shear truss connectors under axial load: preliminary result". Advanced Materials Research. September 2013. Vol. 795. p. 190-194. DOI: https://doi.org/10.4028/www.scientific.net/amr.795.190

[7] Benayoune A, Samad AAA, Ali AAA, Trikha DN. "Response of pre-cast reinforced composite sandwich panels to axial loading". Construction and Building Materials. March 2007. Vol.21-3. p. 677-685. DOI: http://dx.doi.org/10.1016/j.conbuildmat.2005.12.011

[8] Benayoune A, Samad AAA, Trikha DN, Ali AAA, Ellinna SHM. "Flexural behavior of pre-cast concrete sandwich composite panel-Experimental and theoretical investigations". Construction and Building Materials. April 2008. Vol. 22-4. p. 580-592. DOI: https://doi.org/10.1016/j.conbuildmat.2006.11.023

[9] Ye YH, Sun R, Xue ZH, Wang H. "Experimental study on seismic precast NC composite behavior of SCC and shear wall". Journal of Building Structures. July 2014. Vol. 35-7. p. 138-144. DOI: http://dx.doi.org/10.14006/j.jzjgxb.2014.07.017

[10] Bagheri B, Oh SH. "Seismic design of coupled shear wall building linked by hysteretic dampers using energy based seismic design". International Journal of Steel Structures. March 2018. Vol. 18-1. p. 225-253.

[11] Beko A, Rosko P, Wenzel H, Pegon P, Markovic D, Molina FJ. "RC shear walls: Full-scale cyclic test, insights and derived analytical model". Engineering Structures. November 2015. Vol. 102 p. 120-131. DOI: http://dx.doi.org/10.1016/j.engstruct.2015.07.053

[12] Wang ZJ, Li XM, Wang Y, Xu QF, Zhai WH. "Experimental study on seismic behavior of reinforced concrete composite shear wall with confined boundary member". Journal of Central South University (Science and Technology). August 2016. Vol. 47-8. p. 2759-2767. DOI: http://dx.doi.org/10.11817/j.issn.1672-7207.2016.08.030

[13] Wang MF, Zou TQ. "Experimental Study on seismic behavior of precast composite shear wall with concealed bracing". Journal of Hunan University (Natural Sciences). January 2017. Vol. 44-1. p. 54-64. DOI: http://dx.doi.org/10.16339/j.cnki.hdxbzkb.2017.01.008

[14] Chu MJ, Liu JL, Hou JQ, Liu MH, Wang G, Qiu GM. "Experimental study on mechanical behavior of superimpose slab shear walls without interface steel". Journal of Building Structures. October 2016. Vol. 37-10. p. 90-97. DOI: http://dx.doi.org/10.14006/j.jzjgxb.2016.10.011

[15] Song XR, Liu PG, Zhao DF, Qu YT, Zhang XY. "Study on stay-in-place cement formwork and the application". Advanced Materials Research. December 2011, Vol. 163-167. p. 952-955. DOI: https://doi.org/10.4028/www.scientific.net/amr.163-167.952

[16] Song XR, Qu YT, Zhang XY, Niu W, Jiang YF. "Design and analysis of the support system for cement-base formwork". Advanced Materials Research. October 2011. Vol. 374-377. p. 1249-1253. DOI: https://doi.org/10.4028/www.scientific.net/amr.374-377.1249

[17] Bin W, Jiang HJ, Lu XL. "Experimental and numerical investigations on seismic behavior of steel truss reinforced concrete core walls". Engineering Structures. June 2017. Vol. 140. p. 164-176. DOI: https://doi.org/10.1016/j.engstruct.2017.02.055

[18] Nie JG, Hu HS, Fan JS, Tao MX, Li SY, Liu FJ. "Experimental study on seismic behavior of high-strength concrete filled double-steel-plate composite walls". Journal of Constructional Steel Research. September 2013. Vol. 88. p. 206-219. DOI: https://doi.org/10.1016/j.jcsr.2013.05.001

[19] Lu XL, Zhang Y, Zhang HM, Zhang HS, Xiao RJ. "Experimental study on seismic performance of steel fiber reinforced high strength concrete composite shear walls with different steel fiber volume fractions". Engineering Structures. September 2018. Vol. 171. p. 247-259. DOI: https://doi.org/10.1016/j.engstruct.2018.05.068

[20] Huang ST, Huang YS, He A, Tang XL, Chen QJ, Liu XP, Cai J. "Experimental study on seismic behaviour of an innovative composite shear wall". Journal of Constructional Steel Research. September 2018. Vol. 148. p. 165-179. DOI: https://doi.org/10.1016/j.jcsr.2018.05.003

[21] Ren FM, Chen JW, Chen GM, Guo YX, JiangT. "Seismic behavior of composite shear walls incorporating concrete-filled steel and FRP tubes as boundary elements". Engineering Structures. August 2018. Vol. 168. p. 405-419. DOI: https://doi.org/10.1016/j.engstruct.2018.04.032

[22] Wang MF, Wang YJ. "Study on seismic performance of high damping concrete coupled shear walls with concealed steel plate bracings". Engineering Mechanics. January 2017. Vol. 34-1. p. 204-212. DOI: http://dx.doi.org/10.6052/j.issn.1000-4750.2015.07.0543

[23] Dong HY, Cao WL, Wu HP, Zhang JW, Xu FF. "Analysis and seismic tests of composite shear walls with CFST columns and steel plate deep beams". Earthquake Engineering and Engineering Vibration. December 2013. Vol. 12-4. p. 609-624. DOI: https://doi.org/10.1007/s11803-013-0201-1

ACKNOWLEDGEMENTS

This work is financially supported by National Natural Science Foundation of China (51208006) and The Fundamental Research Funds for Beijing Universities (110052971921/059)

SUPPLEMENTARY MATERIAL

https://www.revistadyna.com/documentos/pdfs/_adic/9192-1.pdf